Journal of Natural Sciences Research www.iiste.org
ISSN 2224-3186 (Paper) ISSN 2225-0921 (Online)
Vol.5, No.22, 2015

The Effect of Kelvin Effect on the Equilibrium Effective Radii and Hygroscopic Growth of Atmospheric Aerosols

B.I. Tijjani[1] G.S.M. Galadanci[1] A.I. Abubakar[2] F. S. Koki[1] I. D. Adamu[1] A. M. Nura[1] M. Saleh[1] S. Uba[3]
1. Department of Physics, Bayero University, Kano. NIGERIA
2. Department of Physics, Kano University of Science and Technology, Wudil. NIGERIA
3.Department of Physics, Ahmadu Bello University, Zaria

Abstract
In this paper we extracted microphysical properties of six types of atmospheric aerosols from Optical Properties of Aerosols and Clouds (OPAC) and numerically analyzed the analytical expressions for the changes in the equilibrium relative humidity (RH), effective radius, effective hygroscopic growth, the magnitudes and fractional changes in the effective radii and the effective hygroscopic growth on the effects of surface tension (the Kelvin effect) on ambient atmospheric aerosols. The expressions were applied to two - one parameter models. We discovered from the analysis of the data extracted that, to the lowest order error, the change in the equilibrium RH, effective radii and effective hygroscopic growth depend on the compositions of the aerosols. From the two models used, we also discovered that the fractional changes in the ambient RH, effective radii and effective hygrosocopic growth, also depend on the aerosols compositions. Finally, we discovered that the magnitude of the Kelvin effect and its consequences on the atmospheric aerosols depend on the hygroscopicity of the aerosols.
Keywords: Kelvin effect, effective radius, effective hygroscopic growth, atmospheric aerosols, ambient Relative Humidity.

1. INTRODUCTION

The atmospheric RH in equilibrium with the aqueous solutions of atmospheric aerosols at a given temperature depends on the hygroscopic nature of the solutes, their compositions, concentrations and the effective sizes of these aerosols [1,2]. The continuous variability of these characteristics of these aerosols with the ambient RH automatically affect their surface activities and can influence climate by changing the effective surface tensions of water and can result in changes in cloud droplet concentrations and consequently change in cloud albedo [3,4]. Chemical compositions of aerosol particles released from natural and anthropogenic sources are also not homogeneous either locally or globally, hence characteristics such as hygroscopicity and surface tension are significantly different from one particle to another, controlling the particle's ability to form cloud droplets and also their ability to act as cloud condensation nuclei (CCN). Aerosols that act as cloud condensation nuclei (CCN) to form new cloud droplets usually contain high amount of hygroscopic components and are within effective the size ranges of 0.1-1.0 μm [5].

The equation that is often used to describe both hygroscopic growth of aerosol particles and their activation to cloud droplets is the Kohler equation which is divided into two as: (1) the Kelvin effect; this is responsible for the increase in equilibrium water vapor pressure over a curved surface, and is directly proportional to the effective surface tension as a result of the solution–air interface [6]. For an aqueous solution drop with given concentration, the equilibrium fractional relative humidity increases with decreasing drop radius; and (2) the Raoult effect; this is the reduction in water activity associated with solute dissolution in terms of either effective hygroscopic growth and/or the effective radius of the mixtures at given RHs.

Theoretically, cloud droplet formation is enhanced by the dissolutions of water soluble aerosols and the reduction in surface tension by surface-active materials. A sensitivity study for the prediction of cloud droplet numbers dealing with the above factors suggests that variabilities in the chemical compositions of aerosol particles strongly contribute to the variability of cloud droplet numbers [7]. The importance of reduction of surface tension has been discussed by several researchers [8,9]. However, attempts to measure the surface tension of real particles in the atmosphere are limited [3,4,9,10,11] , and insufficient to estimate the surface tension of atmospheric aerosol particles under various conditions. Further, a lack of information on the bulk hygroscopicity (i.e., solute effect) of the aerosols also limits the prediction of cloud droplet formation. Only one constant value of hygroscopicity has been applied in global models dealing with direct and/or indirect effects of organic aerosols [12,13] despite the fact that the effective hygroscopicity of these aerosols vary depending on their sources and ages [14].

This paper examines the effects of Kelvin effects, the quantities it depends on and its effect on effective radii and effective hygroscopic growth on six types of atmospheric aerosols extracted from OPAC at eight RHs of 0, 50, 70, 80, 90, 95, 98, and 99%. The atmospheric aerosols extracted are Antarctic, Arctic, Continental Clean, Desert, Maritime Clean and Urban. The microphysical properties extracted are the individual aerosols radii and their volume mix ratios. The analytical expressions derived by Lewis [15] for the changes in

the equilibrium radius of a solution drop, the hygroscopic growth, estimates in the changes of their magnitudes and their fractional changes due to the Kelvin effect with dependences on surface tension, particle sizes are numerically analyzed. We then applied the expressions to two known one parameter models. They are the power law dependence (γ-model) and the model as proposed by Petters and Kreidenweis [16].

2. METHODOLOGY

The models extracted from OPAC are given in Table 1.

Table 1 Compositions of aerosols types at 0% RH [17].

S/N	Aerosols Model Types	Aerosols Comp.	No. Conc. (cm^{-3})	R_{min} (μm)	R_{max} (μm)	sigma	R_{mod} (μm)
1	Antarctic	ssam(sol)	0.0470	0.005	20.00	2.03	0.2090
		mitr(ns)	0.0053	0.020	5.00	2.20	0.5000
		suso(sol)	42.9000	0.005	20.00	2.03	0.0695
2	Arctic	inso(ns)	0.0100	0.005	20.00	2.51	0.4710
		waso(sol)	1,300.0000	0.005	20.00	2.24	0.0212
		soot(ns)	5,300.0000	0.005	20.00	2.00	0.0118
		ssam(sol)	1.9000	0.005	20.00	2.03	0.2090
3	Cont. Clean	waso(sol)	2,600.0000	0.005	20.00	2.24	0.0212
		inso(ns)	0.1500	0.005	20.00	2.51	0.4710
4	Desert	waso(sol)	2,000.0000	0.005	20.00	2.24	0.0212
		minm(ns)	269.5000	0.005	20.00	1.95	0.0700
		miam(ns)	30.5000	0.005	20.00	2.00	0.3900
		micm(ns)	0.1420	0.005	60.00	2.15	1.9000
5	Maritime Clean	waso(sol)	1,500.0000	0.005	20.00	2.24	0.0212
		ssam(sol)	20.0000	0.005	20.00	2.03	0.2090
		sscm(sol)	0.0032	0.005	60.00	2.03	1.7500
6	Urban	waso(sol)	28,000.000	0.005	20.00	2.24	0.0212
		inso(ns)	1.5000	0.005	20.00	2.51	0.4710
		soot(ns)	130,000.00	0.005	20.00	2.00	0.0118

The *sol* and *ns* show that the aerosols are soluble and insoluble respectively, the *inso* represents the *water-insoluble* part of aerosol particles and consists mostly of soil particles with a certain amount of organic material. The *waso* represents the *water-soluble* part of aerosol particles that originates from gas to particle conversion and consists of various kinds of sulfates, nitrates, and other, also organic, water-soluble substances. Thus it contains more than only the sulfate aerosol that is often used to describe anthropogenic aerosol. The *soot* component is used to represent absorbing black carbon. Carbon is not soluble in water and therefore the particles are assumed not to grow with increasing relative humidity. The *ssam* and *sscm are Sea-salt accumulation and coarse modes* particles that consist of the various kinds of salt contained in seawater. *Mineral* aerosol or desert dust is produced in arid regions. It consists of a mixture of quartz and clay minerals and is modeled with three modes to allow and consider increasing relative amount of large particles for increasing turbidity. The *mitr* are *Mineral transported,* is used to describe desert dust that is transported over long distances with a reduced amount of large particles. Mineral aerosol particles are assumed not to enlarge with increasing relative humidity. The *suso* is *sulfate* component (75% H_2SO_4) is used to describe the amount of sulfate found in the Antarctic aerosol. Mineral (nucleation mode) MINM, Mineral (accuumulation mode) MIAM, and Mineral (coarse mode) MICM, are mineral aerosols or desert dusts that are produced in arid regions. They consist of mixtures of quartz and clay minerals and are modeled with these three modes to allow considering increasing relative amount of large particles for increasing turbidity

The Kelvin effect and water activity are the major parameters that made hygroscopic growth of aerosols to be size and composition dependent. The growth of aqueous droplets in ambient RH is commonly described by Köhler theory [1,18,19]. According to Kohler theory, the equilibrium water vapor saturation ratio S is given by

$$S=a_wK_e \quad (1)$$

where a_w denotes the water activity or Raoult term, and K_e is the Kelvin effect.
The relationship between droplet radius and RH at equilibrium can also be given as:

$$S = a_w exp\left(\frac{2\sigma v_w}{RT\, r(S)}\right) \quad (2)$$

where v_w is the partial molar volume of water, σ is the surface tension of the solution at the composition of the droplet, R is the universal gas constant, T is the temperature and r(S) is the equilibrium radius.

For single-solute particles, the equilibrium water vapor saturation ratio S for a droplet can be described by [20]:

$$lnS = \frac{A}{r(S)} - \frac{Br^3(S=0)}{r^3(S) - r^3(S=0)} \quad (3)$$

where $A = \frac{2\sigma v_w}{RT}$ and $B = \nu\phi\frac{v_w}{v_s}$ are assumed to be constant, r(s) and r(s=0) are the radii of the mixtures or the volume equivalent radii of the wet and dry mixtures, respectively, σ is the surface tension, v_w and v_s are the molar volumes of pure water and solute, respectively, ν is the degree of dissociation, and ϕ is the osmotic coefficient. The product of ν and ϕ is equivalent to the so-called van't Hoff factor [21], R and T are the gas constant and temperature, respectively.

The aerosol's hygroscopic growth factor g(S), [22,23] is defined as:

$$g(S) = \frac{r(S)}{r(S=0)} \quad (4)$$

where S is taken for eight values 0%, 50%, 70%, 80%, 90%, 95%, 98% and 99% RH.

Substituting equation (4) into equation(3) we obtain

$$lnS = \frac{A}{r(S)} + \frac{B}{1-(g(S))^3} \quad (5)$$

Comparing the first term on the right hand side of equation (5) with equations (1) and (2), we get

$$lnK_e = \frac{2\sigma v_w}{RTr(S)} = \frac{r_K}{r(S)} = g_\sigma(r(S)) \quad (6)$$

where a characteristic length for the effect of surface tension (or Kelvin radius) $r_K = \frac{2v_w\sigma}{RT} = A$, and $g_\sigma(r(S)) = \frac{r_K}{r(S)}$. From equation (6), it can be observe that the Kelvin effect will be small for large droplet radii and becomes very large for radii $r(S)$ smaller than the Kelvin radius r_K.

Now comparing the second term on the right hand side of equation (5) with equation (1) and (2), we get

$$lna_w = \frac{B}{1-(g(S))^3} \quad (7)$$

But generally atmospheric aerosols usually comprised mixtures of soluble and insoluble components, therefore the information on the hygroscopicity modes was merged into an "over-all" or "bulk" or "effective" hygroscopic growth factor of the mixture, g_{eff}(S), representative for the entire aerosols particle population as:

$$g_{eff}(S) = (\sum_k x_k g_k^3(S))^{1/3} \quad (8)$$

The effective or volume equivalent radius of the mixture was determined using the relation

$$r_{eff}(S) = (\sum_k x_k r_k^3)^{1/3} \quad (9)$$

where the summation is performed over all compounds present in the particles and x_k represent their respective volume fractions, using the Zdanovskii-Stokes-Robinson relation [24,25,26,27].

Therefore for atmospheric aerosols, equation (5) can be written to represents the property of the bulk components using equations (8) and (9) as:

$$lnS = \frac{A}{r_{eff}(S)} + \frac{B}{1-g_{eff}^3(S)} \quad (10)$$

using multiple regression analysis with SPSS 16.0 for windows, the constants A and B were determined.

The first term on the right hand side of equation (10) can replace equation (6) as

$$lnK_e = \frac{2\sigma v_w}{RTr_{eff}(S)} = \frac{r_K}{r_{eff}(S)} = g_\sigma\left(r_{eff}(S)\right) \quad (11a)$$

This implies

$$K_e = exp\left(g_\sigma\left(r_{eff}(S)\right)\right) \quad (11b)$$

Where a characteristic length for the effect of surface tension on the mixture or the effective Kelvin radius $r_K = \frac{2v_w\sigma_{eff}}{RT} = A$ and $g_\sigma\left(r_{eff}(S)\right) = \frac{r_K}{r_{eff}(S)} = \frac{A}{r_{eff}(S)}$.

The second term on the right hand side of equation (10) is

$$lna_w = \frac{B}{1-g_{eff}^3(S)} \quad (12a)$$

This implies, $$a_w = exp\left(\frac{B}{1-g_{eff}^3(S)}\right) \quad (12b)$$

The parameter B was described as the bulk hygroscopicity factor under subsaturation conditions [20].
From equations (11) and (12), equation (1) for multiple components can be written as

$$S\left(g_{eff}, g_\sigma(r_{eff})\right) = a_w(g_{eff})exp[g_\sigma(r_{eff})] \quad (13)$$

The error to the first order on ambient RH due to the effect of Kelvin effect on equation (13) was determined by Lewis [15] as :

$$\Delta S\left(g_{eff}, g_\sigma(r_{eff})\right) = S\left(g_{eff}, g_\sigma(r_{eff})\right) g_\sigma(r_{eff}) \quad (14)$$

The lowest correction on the effective hygroscopic growth due to the Kelvin effect was also obtained by Lewis [15] as:

$$\Delta g_{eff}\left(S, g_\sigma(r_{eff})\right) = -\frac{r_K}{r_{eff}(0,0)} \frac{S}{g_{eff}(S,0)} \frac{dg_{eff}(S,0)}{dS}, \quad (15)$$

Similarly, the lowest-order correction to the effective radii due to the Kelvin effect was determined by Lewis [15] as:

$$\Delta r_{eff}(S, g_\sigma) = -r_K \frac{S}{g_{eff}(S,0)} \frac{dg_{eff}(S,0)}{dS} \quad (16)$$

Important observation that can be made from equations (15) and (16) are that, as r_{eff} and g_{eff} are directly dependent on the ambient RH, the corrections will be negative, implying that the effective radii and the effective hygroscopic growth and their ratios calculated from the bulk solution properties will be overestimated. It can also observe that for a given bulk solution the quantities $g_{eff}(S,0)$ and $\frac{dg_{eff}(S,0)}{dS}$, and r_K, depend only on the ambient RH (and weakly on temperature). Thus, to the lowest order, the decrease or increase in the effective radii and hygroscopic growths, resulting from the Kelvin effect and water activity for a given bulk solute depends only on the relative humidity and is independent of $r_{eff}(0,0)$ [15].

The first model was used to determine the Kelvin effect is the empirical γ-model that was used in a lot of literatures [28,29,30,31,32,33,34,5,36,37] to describe the hygroscopic growth of atmospheric aerosol particles as:

$$g_{eff}(S,0) = (1-S)^{-n} \quad (17)$$

where the values of *n* depends on the type of solutes and on the range of relative humidity; and is typically in the range 0.20–0.33, taking values near 1/3 for S near unity, consistent with vapor-pressure lowering given by Raoult's Law [38].
To evaluate equations (15) and (16) for the model given by equation (17), we used the following relations which were determined by us and Lewis [15] as:

$$\Delta g_{eff}\left(S, g_\sigma(r_{eff})\right) = -\frac{r_K}{r_{eff}(0)} \frac{nS}{1-S}. \quad (18)$$

and

$$\Delta r_{eff}\left(S, g_\sigma(r_{eff})\right) = -r_K \frac{nS}{1-S} \quad (19)$$

We determined the fractional changes in the effective hygroscopic growth and effective radii due to the Kelvin effect from equations (18) and (19) as:

$$\frac{\Delta g_{eff}\left(S, g_\sigma(r_{eff})\right)}{g_{eff}(S,0)} = -\frac{r_K}{r_{eff}(0)} \frac{nS}{(1-S)^{1-n}} \quad (20)$$

And $$\frac{\Delta r_{eff}(S, g_\sigma)}{r_{eff}(S,0)} = -\frac{r_K}{r_{eff}(S)} \frac{nS}{1-S} \quad (21)$$

The second model is the relation between $g_{eff}(S,0)$ and S that has been parameterized in a good approximation by

a one-parameter equation, proposed e.g. by Petters and Kreidenweis [16], the k-model, Gysel et al., [39] and used extensively by some researches [33,34,35,36,37] as:

$$g_{eff}(S,0) = \left(1 + \kappa \frac{S}{1-S}\right)^{\frac{1}{3}} \quad (22)$$

The coefficient κ is a simple measure of the particle's hygroscopicity and captures all solute properties (Raoult effect), that is, it is for the ensemble of the particle which can be defined in terms of the sum of its components. In an ensemble of aerosol particles, the hygroscopicity of each particle can be described by an "effective" hygroscopicity parameter κ [16,40]. Here "effective" means that the parameter accounts not only for the reduction of water activity by the solute but also for surface tension effects [41,42]. It also scales the volume of water associated with a unit volume of dry particle [16] and depends on the molar volume and the activity coefficients of the dissolved compounds [43].

Evaluation of equations (15) and (16) for the model given by equation (22) we determined :

$$\Delta g_{eff}\left(S, g_\sigma(r_{eff})\right) = -\frac{Sk}{3(1-s)^2}\frac{r_K}{r_{eff}(0,0)}\left(1 + \frac{kS}{1-S}\right)^{-1} \quad (23)$$

and

$$\Delta r_{eff}(S, g_\sigma) = -\frac{Sk\ r_K}{3(1-s)^2}\left(1 + \frac{kS}{1-S}\right)^{-1} \quad (24)$$

From equation (22) the fractional change in the effective hygroscopic growth factor and effective radii due to the Kelvin effect were determined using equations (23) and (24) as

$$\frac{\Delta g_{eff}\left(S, g_\sigma(r_{eff})\right)}{g_{eff}(S,0)} = -\frac{Sk}{3(1-s)^2}\frac{r_K}{r_{eff}(0,0)}\left(1 + \frac{kS}{1-S}\right)^{-4/3} \quad (25)$$

$$\frac{\Delta r_{eff}(S, g_\sigma)}{r_{eff}(S,0)} = -\frac{Skr_K}{3r_{eff}(S,0)(1-s)^2}\left(1 + \frac{kS}{1-S}\right)^{-1} \quad (26)$$

The fractional change in the equilibrium pressure $S\left(g_{eff}, g_\sigma(r_{eff})\right)$ due to the error in Kelvin effect on equation (14) was determined as

$$\frac{\Delta S\left(g_{eff}, g_\sigma(r_{eff})\right)}{S\left(g_{eff}(S,0),0\right)} = \frac{S\left(g_{eff}, g_\sigma(r_{eff})\right)}{S\left(g_{eff}(S,0),0\right)} g_\sigma(r_{eff}) \quad (27)$$

where $S\left(g_{eff}(S,0),0\right)$ is the actual RH.

RESULTS AND DISCUSSIONS

Table 2: The results of the regression of equation (10), the critical water vapor of super saturation using equation (28), the effective radii of the aerosols at 0% RH using equation (9) and the percentage by volume of water soluble components of the aerosols.

	equation (10)			*Equa (9)*	
equ 10	R^2	A (Kelvin radii) (μm)	B (Bulk hygroscopicity factor)	r_{eff} (μm) at 0% RH	% vol. of water solubles
Antarctic	0.9957	0.0221	1.4648	0.1916	94.82
Arctic	0.9957	0.0268	1.5819	0.2075	79.22
Cont. Clean	0.9970	0.0066	0.4125	0.3685	52.12
Mari. Clean	0.9893	0.0512	2.1480	0.5926	100.00
Sahara	0.9990	-0.0186	0.0194	1.1284	1.71
Urban	0.9979	0.0054	0.3727	0.3421	44.93

From table 2, it can be seen that, from the values of R^2, that the data fitted the equation very well. By comparing A(Kelvin radii) and B (Bulk hygroscopicity factor) with the effective radii of the aerosols at 0%, it can be observe that they don't depend on the initial size of the radii. But by analysing their compositions from table 1, it can be seen that both A and B depend on the nature of the compositions. From the values of Kelvin radii, it can be seen that it is negative for the Saharan aerosols. It can be concluded that, the Kelvin radii, apart from positive for concave curvature and zero for flat surface, but it can also be negative which can be called as convex curvature. By comparing the values of the effective radii at 0% RH, the Kelvin radii and the Bulk hygroscopicity factor, it can be concluded that the most important parameter in the formula is the Kelvin radii.

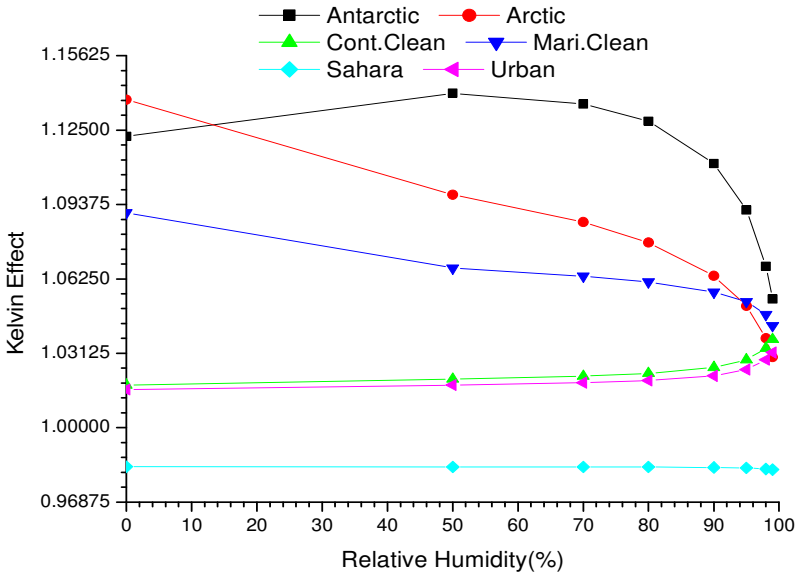

Figure 1: A plot of Kelvin effect of the aerosols against Relative Humidity using equation (11b).

From figure 1, it can be seen that Kelvin effect on the Saharan aerosols is independent of RH (that is it is constant) and is less than 1. Secondly, the urban and continental clean have the same type of behavior, in that they increase slightly with the increase in RH and are slightly more sensitive at higher RHs (95 to 99). Lastly, the remaining are more sensitive to RH although the sensitivity increases with increase in RH in a non-linear form. By comparing figure 1, with table 2, it can be observe that apart from high percentage of hygroscopic solutes, the next important parameter that effect Kelvin effect is the effective radii, that is, the smaller the effective radii the higher the Kelvin effect.

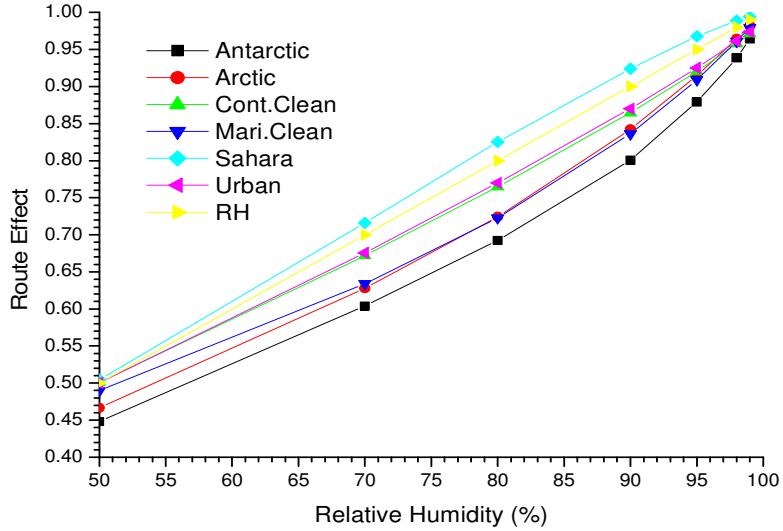

Figure 2: A plot of Route effect (water activity) of the aerosols against Relative Humidity using equation (12b).

From figure 2, the plot of RH which is the ambient RH is used to compare how the Route effects affect the ambient RH for the aerosols. From the figure it can be seen that Route effect lowers the ambient RH of Arctic, Antarctic, Maritime clean, Urban and continental clean, while it raised that of Saharan aerosols. By comparing the plots in the figure with the values of r_{eff} at 0% RH and % by volume of water soluble from table 2, it can be observe that the route effect is higher for the aerosols that are very hygroscopic and smallest effective radii. By comparing figure 2 with the r_{eff} at 0% RH and % by volume of water soluble, it can be observe that, not only the high % of water soluble that is important, but also the effective radii of the mixture.

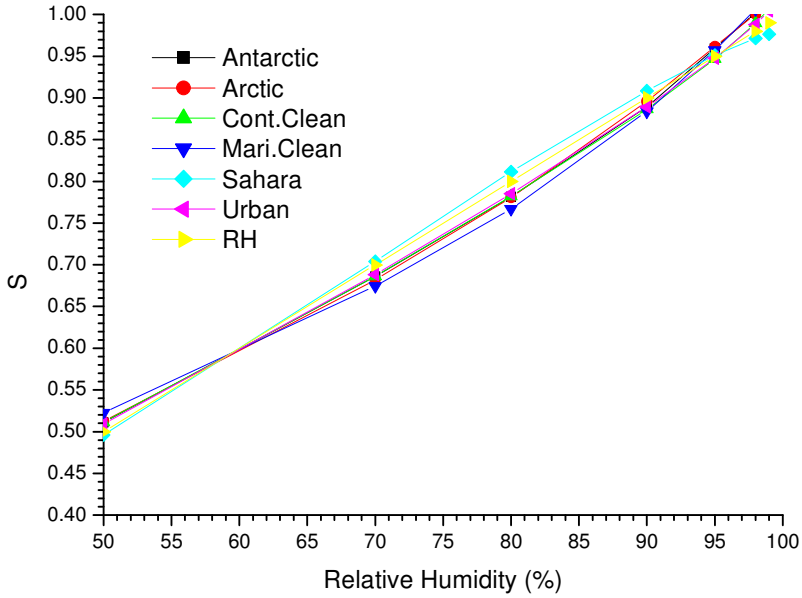

Figure 3: A plot of S(RH) of the aerosols against Relative Humidity using equation (13).

Figure 3 shows the plots of calculated S using equation (13) for the aerosols and the ambient RH. Comparing this figure with figures 1 and 2, it can be seen that for Saharan aerosols, Route effect is more dominant at the RH of 70, 80 and 90%, while for the remaining five aerosol, the Kelvin effects are more dominant at the RH of 50, 95, 98, and 99% RH.

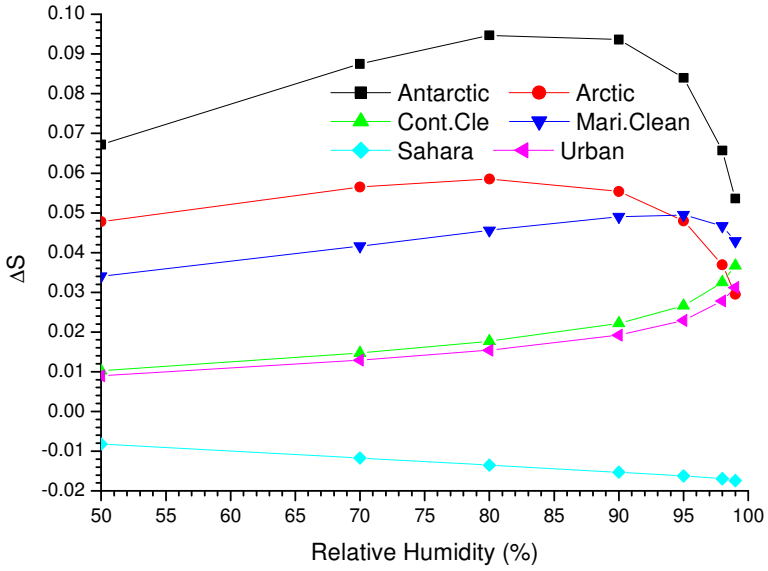

Figure 4: A plot of ΔS of the aerosols against Relative Humidity using equation (14).

Figure 4 shows the plots of the amounts by which the equilibrium RH of the aerosols is larger than the water activity due to the Kelvin effect. From the figure, it can be observe that for Sahara the error in RH shows overestimation and it increases almost linearly with the RH from 0.008 to 0.018. For the remaining five aerosols, we observed some underestimation within 0.008 to 0.095 depending on the type of the aerosols and RHs and the errors are very sensitive to RHs.

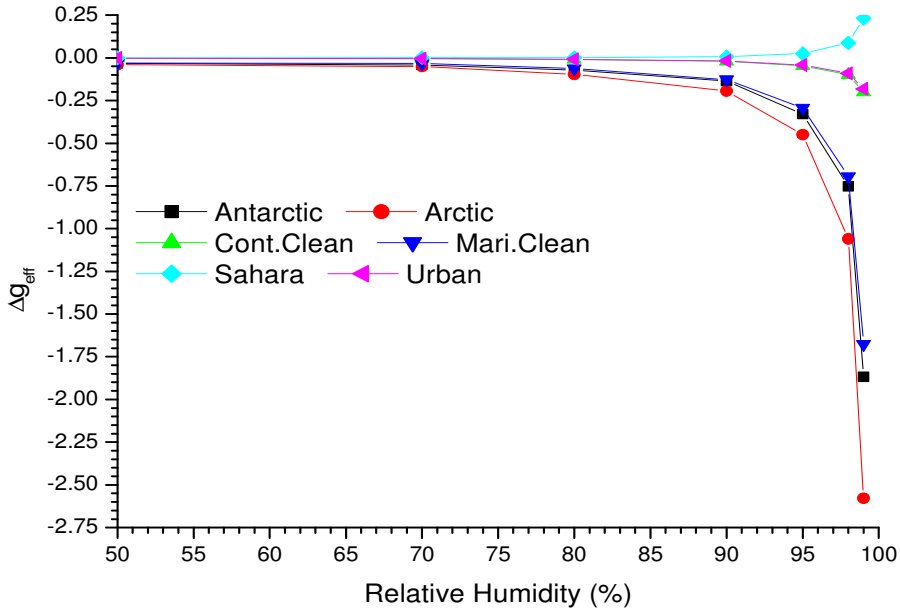

Figure 5: A plot of Δg_{eff} of the aerosols against Relative Humidity using equation (15).

Figure 5 shows the plots of the change or correction in the effective hygroscopic growth due to the Kelvin effect. From the figure, it can be observe that the corrections in the effective hygroscopic growths due to the Kelvin effects are that for five aerosols they are over estimated at different levels, while for Sahara they are underestimated. The errors in the estimations increase in almost exponential or power form with the increase in RH. It also shows that, the estimation depend on the degree of hygroscopicity.

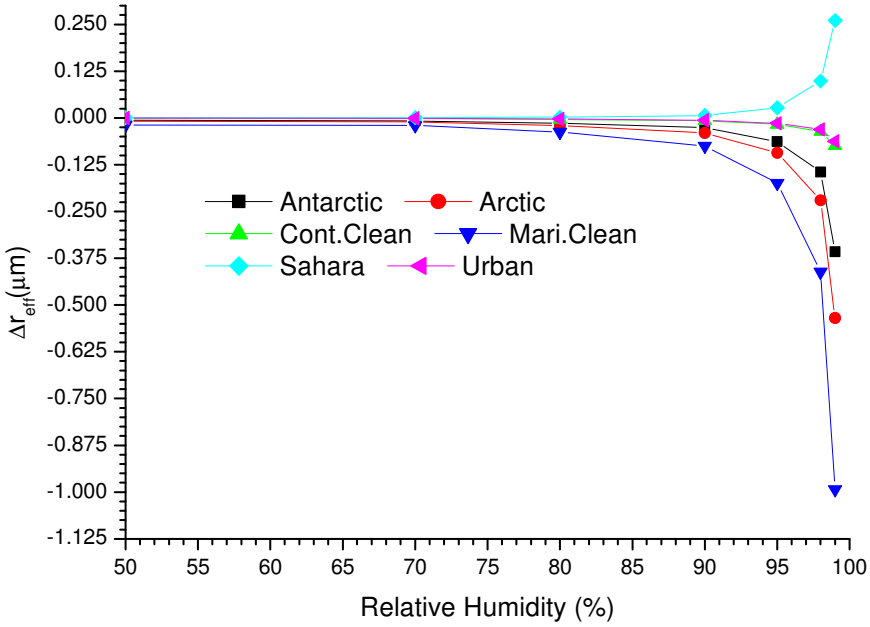

Figure 6: A plot of Δr_{eff} of the aerosols against Relative Humidity using equation (16).

Fgure 6 shows the corrections to the effective radii due to the Kelvin effect. it can be observe that the error corrections in the effective radii due to the Kelvin effect is that for the six aerosols are similar to that of figure 5. However, there is a decrease in the overestimation for five aerosols, while for Sahara there is an increase in the under estimation.

Table 3: Equation (17): The results of the regression of equation (17), using the ambient RHs and the water activity.

	equ17	
	R^2	n
Antarctic	0.9891	0.2816
Arctic	0.9942	0.3317
Cont. Clean	0.9997	0.1981
Mari. Clean	0.9868	0.3544
Sahara	0.8661	0.0766
Urban	0.9995	0.1950

From table 3, by observing the values of R^2, it can be observe that the data fitted the equation very excellent. As determined by Lewis & Randall, (1961), that n is typically in the range 0.20–0.33, taking values near 1/3 for S near unity, it can be observe that, the values of n also depends on the types of the aerosols and compositions.

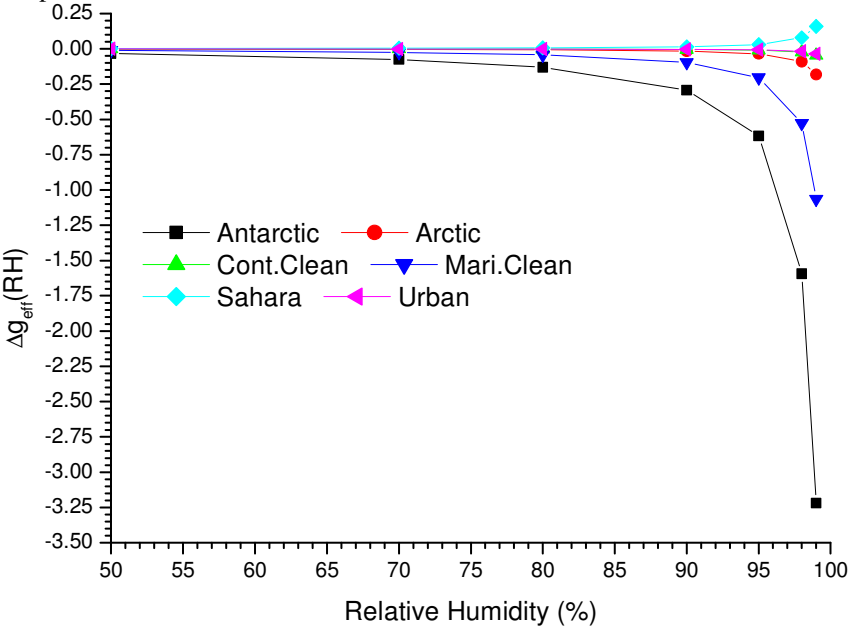

Figure 7: A plot of $\Delta g_{eff}(RH)$ of the aerosols against Relative Humidity using equation (18)

Figures 7 shows the correction to the effective hygroscopic growth due to the Kelvin effect on equation (17) using equation(18) with the increase in RH. From the figure, it can be seen that Antarctic has the highest overestimation followed by Maritime clean, then Arctic. For Urban and continental clean the effect is negligible. However, for Sahara underestimation is observed.

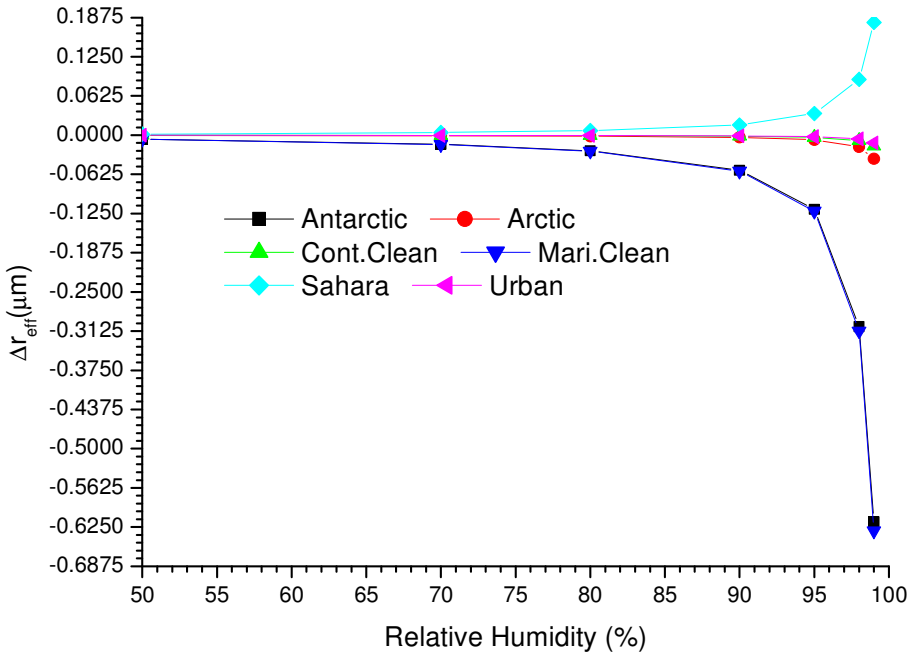

Figure 8 : A plot of $\Delta r_{eff}(RH)$ of the aerosols against Relative Humidity using equation (19).

Figure 8 shows the plots for correction of the effective radii of the aerosols due to Kelvin effect with RH for equation (17) using equation (19). From the figure, it can be observe that the overestimation due to Kelvin effect is higher for Antarctic and Maritime clean and the errors become more important at higher RHs. But for Arctic, Urban and Continental clean, the error is very small, though it becomes higher as from the RHs of 95, 98 and 99. For Sahara, we can see underestimation that is more important at higher RHs.

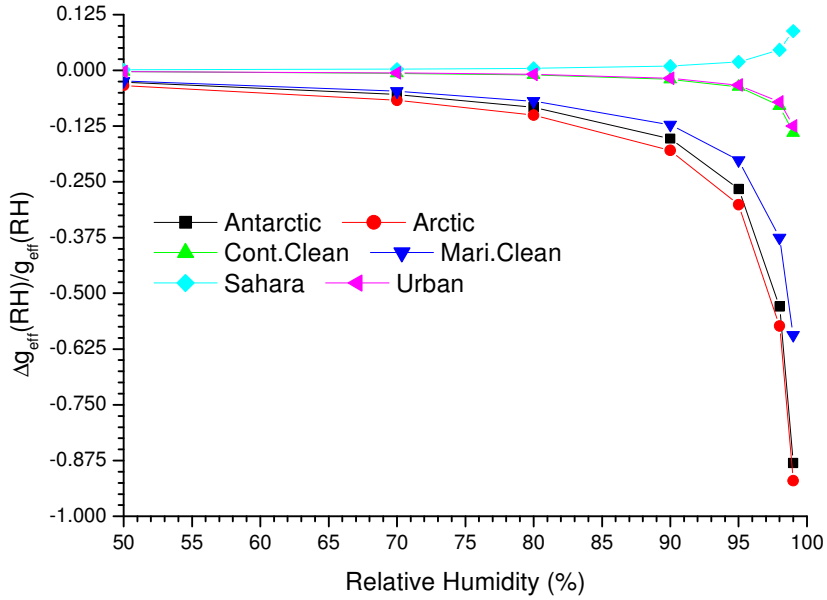

Figure 9: A plot of $\Delta g_{eff}/g_{eff}(RH)$ of the aerosols against Relative Humidity using equation (20).

Figure 9 shows the plots of the fractional change in the effective hygroscopic growth of equation (17) using equation (20). From the plots, it can be observe that Arctic has higher overestimation followed by Antarctic, then Maritime clean followed by Urban and Continental clean, lastly, underestimation can be observe for Sahara. Lastly,comparing this figure with table 2, it can be observe that the higher the percentage of water soluble, the higher the overestimation, most especially at higher RHs.

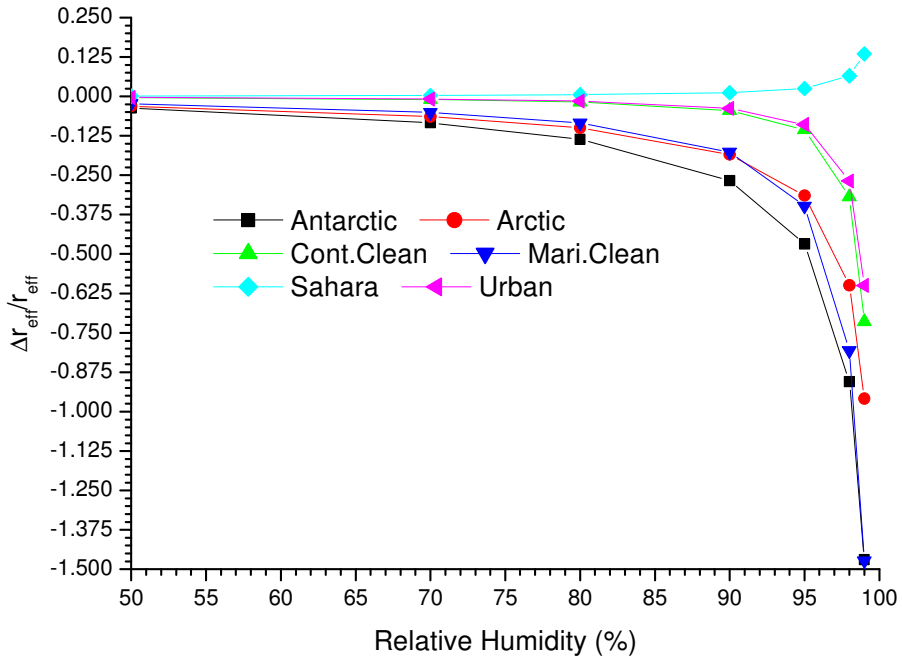

Figure 10: A plot of $\Delta r_{eff}/r_{eff}(RH)$ of the aerosols against Relative Humidity using equation (21).

Figures 10 shows the plots of the fractional change in the effective radii of equation (17) using equation (21). From the plots, it can be observe that Antarctic and Maritime clean have the highest overestimation, followed by Arctic, then Continental clean followed by Urban, but underestimation for Saharan aerosols. All the overestimation and underestimation increased with RH in almost exponential or power form.

Table 3: equation (22): The results of the regression of equation (22), using the ambient RHs the water activity.

	Equation 24	
	R^2	k
Antarctic	0.9837	0.4270
Arctic	0.9992	0.8838
Cont. Clean	0.9610	0.1579
Mari. Clean	0.9980	1.0685
Sahara	0.9991	0.0332
Urban	0.9644	0.1545

From table 3, it can be seen that by observing the values of R^2, it shows that the data fitted the equation very well.

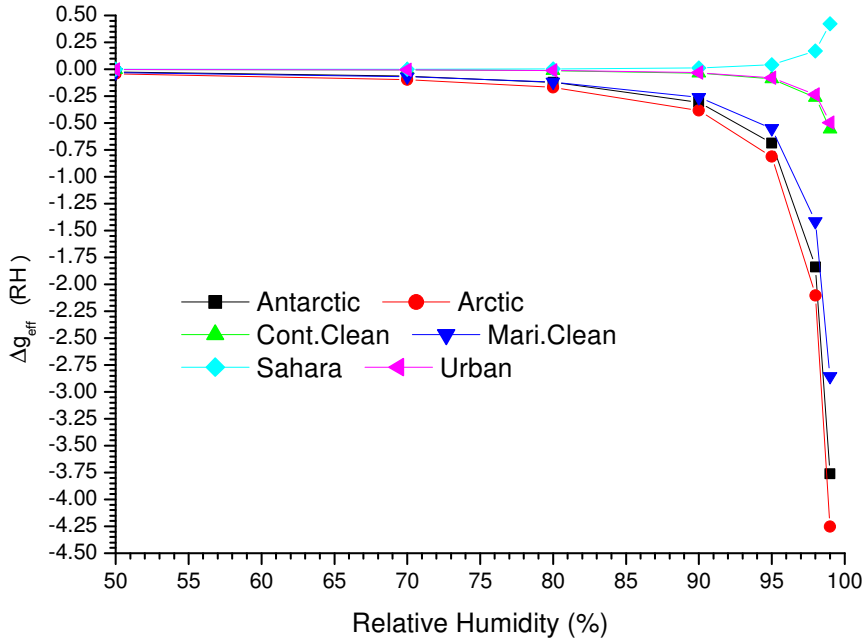

Figure11: A plot of $\Delta g_{eff}(RH)$ of the aerosols against Relative Humidity using equation (23).

Figure 11 shows the correction for the effective hygroscopic growth of equation (22) using equation (23). From the plots, it can be seen that the error in the Kelvin effect with RH has caused decrease in the overestimation of five aerosols, and increase in the underestimation of Sahara.

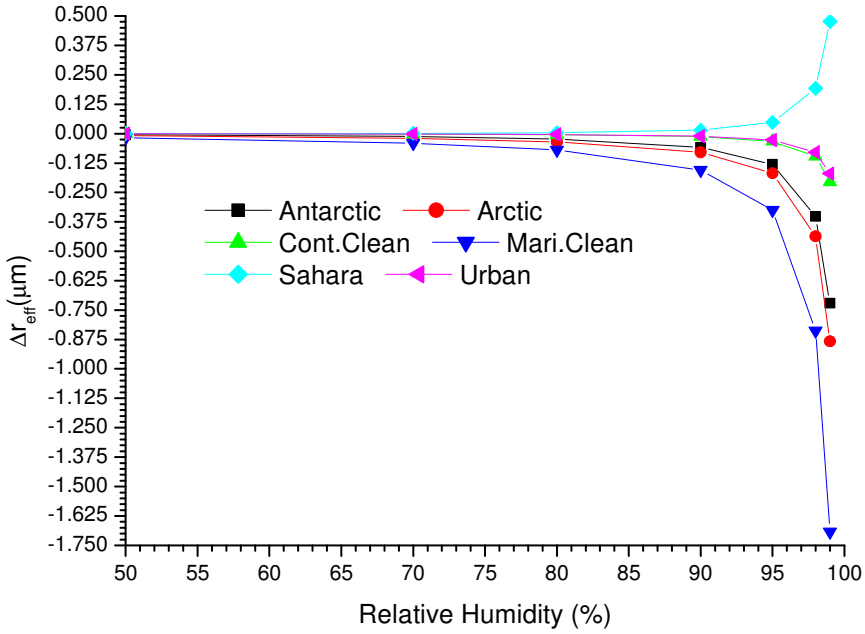

Figure12 A plot of $\Delta r_{eff}(RH)$ of the aerosols against Relative Humidity using equation (24).

Figures 12 shows the plots of the correction to the effective radii due to the Kelvin effect with RHs. From the plots it can be observe that the error in the Kelvin effect with RH has caused decrease in the overestimation for five aerosols, but increase in the underestimation of Sahara.

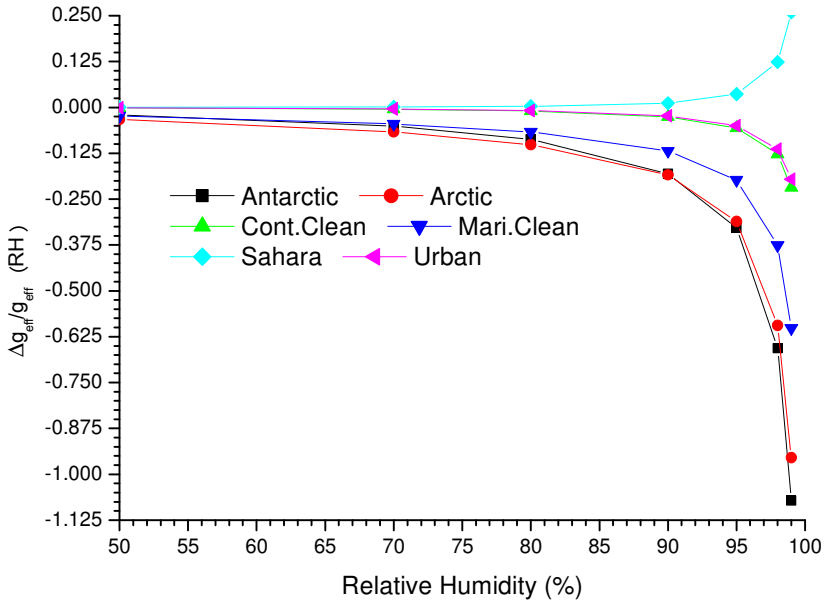

Figure13: A plot of $\Delta g_{eff}/g_{eff}(RH)$ of the aerosols against Relative Humidity using equation (25).

Figures 18 shows the plots of the fractional change in the effective hygroscopic growth of equation (22) using equation (25) due to the Kelvin effect with RHs. The plots show decrease in the over estimation for five aerosols but increase in the under estimation for Sahara aerosols.

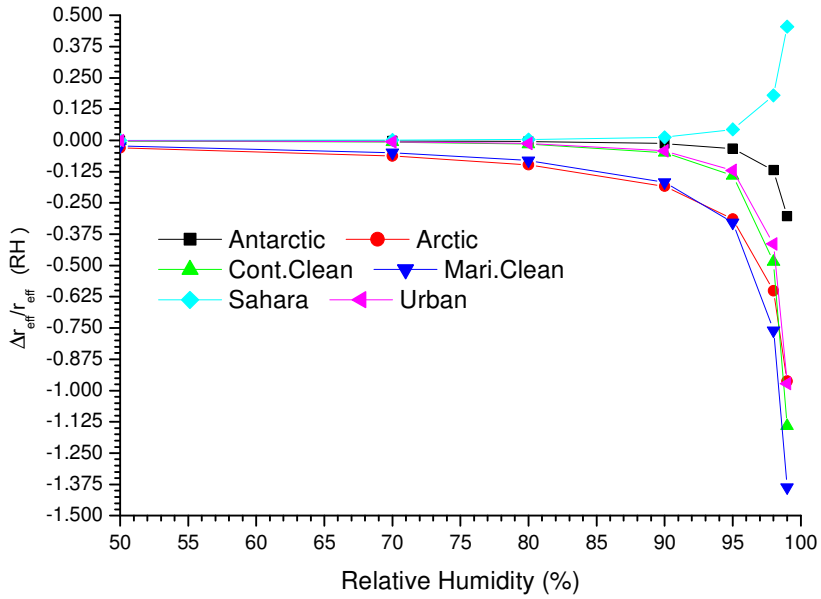

Figure14: A plot of $\Delta r_{eff}/r_{eff}(RH)$ of the aerosols against Relative Humidity using equation (26).

Figures 14 shows the plots of the fractional change in the effective radii of equation (22) using equation (26) due to the Kelvin effect with RHs. The plots show for five aerosols increase in the overestimation but increase in the underestimation for Sahara.

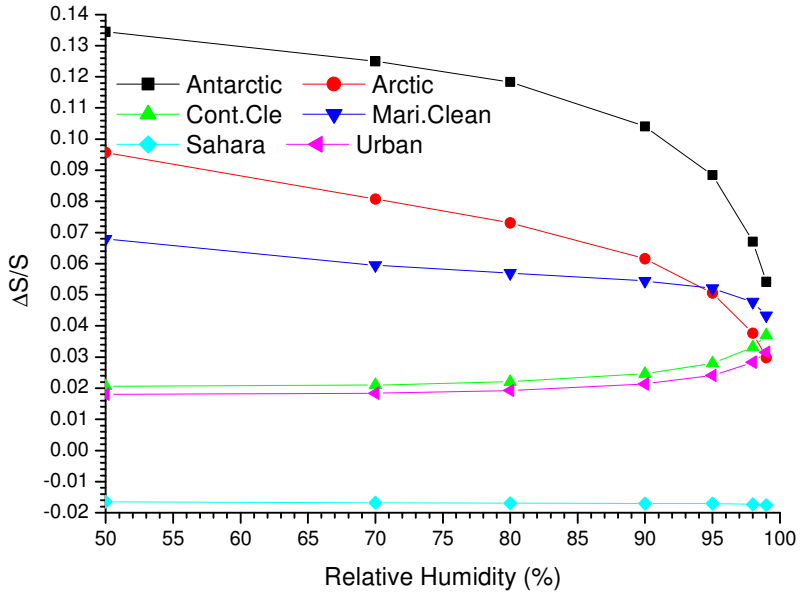

Figure 15: A plot of ΔS/S of the aerosols against Relative Humidity using equation (13) and the ambient RHs.

Figure 15 shows the plots of the fractional change in the RH of equation (13) using equation (27) with the ambient RHs. From the plots, it can be observe that for Antarctic, Arctic and Maritime clean, the errors in the underestimation decreased with the increase in RH, for Continental clean and Urban the errors in underestimation decrease while for Sahara is shows error in the overestimation which is almost constant with RH.

4. CONCLUSION

For lower RHs, (50 and 70) the range of the over estimation and underestimation of the effective hygroscopic growth and effective radii are less that 1% depending on the type of the aerosols. As the RH increases, both the underestimation and the overestimation increase in the form of power law with respect to RH. This implies that there is a strong departure from ideality as the RH increases and this can be attributed to the electrolytic nature of the ionic solutions of the mixtures. This shows that at higher RHs more complicated expressions are required to achieve greater accuracy [15]. This finally shows that Kelvin corrections are necessary for proper modelling of effective hygroscopic growths and effective radii of atmospheric aerosols. From table 2, by looking at the effective radii of the dry aerosols, percentage of water soluble and the s_c, it shows that even atmospheric for the mixture to act as cloud condensation nuclei (CCN) to form new cloud droplets they must contain high amount of hygroscopic components and should be within the effective size ranges of 0.1-1.0 µm as also determined by Solomon et. al., [5]. However, there are some researchers that reported some erroneous implementation of the hygroscopic growth within OPAC, especially at intermediate RH ranges with the exception of Saharan dust [44].

5. REFERENCES

[1] Kohler, H.: (1936). The nucleus in and the growth of hygroscopic droplets. *Transaction of Faraday Society, 32*, 1152–1161.
[2] Wright, H. L. (1936). The size of atmospheric nuclei: Some deductions from measurements of the number of charged and uncharged nuclei at Kew Observatory. *Proceedings of the Physical Society,48(5)*, 675–688.
[3] Facchini, M., M. Mircea, S. Fuzzi, and R. J. Charlson, (1999): Cloud albedo enhancement by surface-active organic solutes in growing droplets. *Nature*, *401*, 257–259. doi:10.1038/45758.
[4] Facchini, M. C., Decesari, S., Mircea, M., Fuzzi, S., and Loglio, G.(2000). Surface tension of atmospheric wet aerosol and cloud/fog droplets in relation to their organic carbon content and chemical composition, *Atmospheric Environment*, *34(28)*, 4853–4857.
[5] Solomon, S., D. Qin, M. Manning, Z. Chen, M., and Marquis, K. A., M. Tignor, and H. Miller (2007). Climate Change 2007: The Physical Science Basis. Contribution of Working Group I to the Fourth Assessment Report of the Intergovernmental Panel on Climate Change., Cambridge University Press, Cambridge, United Kingdom and New York, NY, USA.
[6] Thomson, S. W. (1871). On the equilibrium of vapour at a curved surface of liquid. *Philosophical Magazine Series 4. 42(282)*, 448–452.
[7] Lance, S., A. Nenes, and T. A. Rissman (2004), Chemical and dynamical effects on cloud droplet number: Implications for estimates of the aerosol indirect effect, *Journal of Geophysical Research: Atmospheres*, 109,

D22208. doi:10.1029/ 2004JD004596.
[8] Nenes, A., R. J. Charlson, M. C. Facchini, M. Kulmala, A. Laaksonen, and J. H. Seinfeld (2002), Can chemical effects on cloud droplet number rival the first indirect effect?, *Geophysical Research Letters., 29(17)*, 1848, doi:10.1029/2002GL015295.
[9] Dinar, E., Taraniuk, I., Graber, E. R., Anttila, T., Mentel, T. F., and Rudich, Y. (2007). Hygroscopic growth of atmospheric and model humic-like substances, *Journal of Geophysical Research:Atmospheres*, *112*, 1–13, doi: 10.1029/2006JD007442, 2007.
[10] Asa-Awuku, A., Sullivan, A. P., Hennigan, C. J., Weber, R. J., and Nenes, A. (2008). Investigation of molar volume and surfactant characteristics of water-soluble organic compounds in biomass burning aerosol, *Atmospheric Chemistry and Physics*, *8*, 799–812. http://www.atmos-chem-phys.net/8/799/2008/.
[11] Ovadnevaite, J., D. Ceburnis, G. Martucci, J. Bialek, C. Monahan, M. Rinaldi, M. C. Facchini, H. Berresheim, D. R. Worsnop, and C. O'Dowd (2011), Primary marine organic aerosol: A dichotomy of low hygroscopicity and high CCN activity, *Geophysical Research Letters, 38*, L21806, doi:10.1029/2011GL048869.
[12] Ghan, S., N. Laulainen, R. Easter, R. Wagener, S. Nemesure, E. Chapman, Y. Zhang, and R. Leung (2001a), Evaluation of aerosol direct radiative forcing in MIRAGE, *Journal of Geophysical Research: Atmospheres*, *106*, 5295 – 5316.
[13] Ghan, S., R. Easter, J. Hudson, and F.-M. Bre´on (2001b), Evaluation of aerosol indirect radiative forcing in MIRAGE. *Journal of Geophysical Research: Atmospheres*, *106*, 5317 – 5334.
[14] Saxena, P., Hildemann L. M., McMurry P. H., and Seinfeld J. H. (1995). Organics alter hygroscopic behavior of atmospheric particles, *Journal of Geophysical Research, 100(D9)*, 18,755–18,770.
[15] Lewis E. R. (2006), The effect of surface tension (Kelvin effect) on the equilibrium radius of a hygroscopic aqueous aerosol particle, *Journal of Aerosol Science, 37*, 1605 – 1617, www.elsevier.com/locate/jaerosci.
[16] Petters, M. and Kreidenweis, S.: (2007) A single parameter representation of hygroscopic growth and cloud condensation nucleus activity. *Atmospheric Chemistry and Physics, 7*, 1961–1971, doi:10.5194/acp-7-1961-2007,
[17] Hess M., Koepke P., and Schult I (May 1998), Optical Properties of Aerosols and Clouds: The Software Package OPAC. *Bulletin of the American Meteorological Society, 79*, 5, 831-844.
[18] Gysel, M., Weingartner, E., and Baltensperger, U. (2002): Hygroscopicity of aerosol particles at low temperatures. 2. Theoretical and experimental hygroscopic properties of laboratory generated aerosols. *Environmental Science and Technology, 36*, 63–68.
[19] Kreidenweis S. M., K. Koehler, P. J. DeMott, A. J. Prenni, C. Carrico, and B. Ervens (2005) Water activity and activation diameters from hygroscopicity data –Part I: Theory and application to inorganic salts, *Atmospheric Chemistry Physics, 5*, 1357–1370, www.atmos-chem-phys.org/acp/5/1357/ SRef-ID: 1680-7324/acp/2005-5-1357.
[20] Mochida M., Kuwata M., Miyakawa T., Takegawa N., Kawamura K., and Kondo Y. (2006) Relationship between hygroscopicity and cloud condensation nuclei activity for urban aerosols in Tokyo. *Journal Of Geophysical Research, 111*, D23204, doi:10.1029/2005JD006980.
[21] Pruppacher, H. R., and J. D. Klett (1997),Microphysics of Clouds and Precipitation, 2nd ed., 954 pp., Springer, New York.
[23] Randles , C. A. , Russell L. M. and. Ramaswamy V. (2004). Hygroscopic and optical properties of organic sea salt aerosol and consequences for climate forcing. *Geophysical Research Letters, 31*, L16108, doi:10.1029/2004GL020628.
[24] Sjogren, S., Gysel, M., Weingartner, E., Baltensperger, U., Cubi-son, M. J., Coe, H., Zardini, A. A., Marcolli, C., Krieger, U. K., and Peter, T.(2007): Hygroscopic growth and water uptake kinetics of two-phase aerosol particles consisting of ammonium sulfate, adipic and humic acid mixtures. *Journal of Aerosol Science, 38*, 157–171.
[25] Stokes, R. H. and Robinson, R. A. (1966). Interactions in aqueous nonelectrolyte solutions. I. Solute-solvent equilibria. *Journal of Physical Chemistry, 70*, 2126–2130.
[26] Meyer, N. K., Duplissy, J., Gysel, M., Metzger, A., Dommen, J., Weingartner, E., Alfarra, M. R., Prevot, A. S. H., Fletcher, C., Good, N., McFiggans, G., Jonsson, A. M., Hallquist, M., Baltensperger, U., and Ristovski, Z. D. (2009): Analysis of the hygroscopic and volatile properties of ammonium sulphate seeded and unseeded SOA particles. *Atmospheric. Chemistry and Physics, 9*, 721–732, doi:10.5194/acp-9-721-2009.
[27] Stock M., Y. F. Cheng, W. Birmili, A. Massling, B. Wehner, T. Muller, S. Leinert, N. Kalivitis,N. Mihalopoulos, and A. Wiedensohler, (2011). Hygroscopic properties of atmospheric aerosol particles over the Eastern Mediterranean: implications for regional direct radiative forcing under clean and polluted conditions. *Atmospheric Chemistry and Physics., 11*, 4251–4271, www.atmos-chem-phys.net/11/4251/2011/ doi:10.5194/acp-11-4251-2011
[28] Swietlicki, E., Zhou, J., Covert, D. S., Hameri, K., Busch, B., Vakeva, M., Dusek, U., Berg, O. H., Wiedensohler, A., Aalto, P., Makela, J., Martinsson, B. G., Papaspiropoulos, G., Mentes, B., Frank, G., and

Stratmann, F. (2000). Hygroscopic properties of aerosol particles in the northeastern Atlantic during ACE-2. *Tellus, 52B*, 201–227.
[29] Birmili, W., Nowak, A., Schwirn, K., Lehmann, K.et al. (2004). A new method to accurately relate dry and humidified number size distributions of atmospheric aerosols. *Journal of Aerosol Science*, *1*, 15–16.
[30] Kasten, F. (1969). Visibility forecast in the phase of pre-condensation. *Tellus, XXI, 5*, 631–635.
[31] Gysel, M., McFiggans, G. B., and Coe, H. (2009). Inversion of tandem differential mobility analyser (TDMA) measurements, *Journal of Aerosol Science, 40*, 134–151.
[32] Putaud, J. P. (2012): Interactive comment on "Aerosol hygroscopicity at Ispra EMEP-GAW station" by M. Adam et. al., *Atmospheric Chemistry and Physics, Discussions, 12*, C1316–C1322.
[33] Tijjani B. I. (2013a), The Effect of Soot and Water Soluble on the Hygroscopicity of Urban Aerosols. *Journal of Advances in Physics Theories and Applications, 26*, 52-72.
[34] Tijjani B. I. and Uba S. (2013a), The Effect Of Hygroscopic Growth On Urban Aerosols, (2013). *The International Institute for Science, Technology and Education, 25*, 58-75.
[35] Tijjani B. I. and Uba S. (2013b). The effect of hygroscopic growth on desert aerosols, Pelagia Research Library. *Journal of Advances in Applied Science Research, 4(4)*, 465 -478.
[36] Tijjani B. I., (2013b), The Effect Of Water Solubles On The Hygroscopicity Of Urban Aerosols. *International Journal of Computational Engineering Research, 03(11)*, 45-60.
[37] Tijjani B. I., Aliyu A., Shuaibu F. (2013). The Effect of Hygroscopic Growth on Continental Aerosols. *Open Journal of Applied Sciences, 3*, 381-392; http://dx.doi.org/10.4236/ojapps.2013.36048.
[38] Lewis, G. N., & Randall, M. (1961). Thermodynamics (2nd ed.) (713pp.) (revised by K. S. Pitzer & L. Brewer). *New York: McGraw-Hill Book Company*.
[39] Gysel, M., Weingartner, E., Nyeki, S., Paulsen, D., Baltensperger, U., Galambos, I., Kiss, G., (2004). Hygroscopic properties of water-soluble matter and humic-like organics in atmospheric fine aerosol. *Atmospheric Chemistry and Physics, 4*, 35-50
[40] Sullivan, R. C., S. A. Guazzotti, D. A. Sodeman, and K. A. Prather, 2007: Direct observations of the atmospheric processing of asian mineral dust. *Journal of Atmospheric Chemistry and Physics, 7(5)*, 1213–1236, doi:10.5194/acp-7-1213-2007.
[41] Rose D., Gunthe S. S., Frank G. P., Dusek U., Andreae M. O., and Pöschl U. (2008). Calibration and measurement uncertainties of a continuous-flow cloud condensation nuclei counter (DMT-CCNC): CCN activation of ammonium sulfate and sodium chloride aerosol particles in theory and experiment. *Atmospheric Chemistry and Physics*, *8*, 1115-1179.
[42] Gunthe, S. S., King, S. M., Rose, D., Chen, Q., Roldin, P., Farmer, D. K., Jimenez, J. L., Artaxo, P., Andreae, M. O., Martin, S. T., and P¨oschl, U.(2009). Cloud condensation nuclei in pristine tropical rainforest air of Amazonia: size-resolved measurements and modeling of atmospheric aerosol composition and CCN activity. *Atmospheric Chemistry and Physics*, *9*, 7551–7575, doi:10.5194/acp-9-7551-2009.
[43] Christensen, S. I. and Petters, M. D. (2012). The role of temperature in cloud droplet activation. *Journal of Physical Chemistry A, 116(39),* 9706–9717.
[44] Zieger P., Fierz-Schmidhauser R., Weingartner E. and Baltensperger U. (2013) Effects of relative humidity on aerosol light scattering:results from different European sites. *Journal of Atmospheric Chemistry and Physics, 13*, 10609–10631, www.atmos-chem-phys.net/13/10609/2013/, doi:10.5194/acp-13-10609-2013